Surface and Coatings Technology, 66 (1994) 446–452

Corrosion and mechanical behavior of ion implanted bearing steels for improved fretting behavior

G. S. Was

Department of Nuclear Engineering, Department of Materials Science and Engineering, 213 Cooley Building, University of Michigan, Ann Arbor, MI 48109 (USA)

J. D. Demaree

Materials Research Branch, US Army Materials Test Laboratory, Watertown, MA 02172 (USA)

V. Rotberg

Department of Nuclear Engineering, Michigan Ion Beam Laboratory, 120 NAME Building, University of Michigan, Ann Arbor, MI 48109 (USA)

K. Kim

Department of Mechanical Engineering and Applied Mechanics, 3001 EECS, University of Michigan, Ann Arbor, MI 48109 (USA)

Abstract

Ion implantation of AISI 52100 and 1070 steels was conducted in order to improve the corrosion, wear and ultimately the fretting behavior of the steels. Implantations consisted of 1×10^{17} Ta^+ cm^{-2}, 3×10^{17} Ti^+ cm^{-2} + 1.5×10^{17} C^+ cm^{-2}, and 3.1×10^{17} Ti^+ cm^{-2} + 1.55×10^{17} N_2^+ cm^{-2}. All implantations were successful in improving the corrosion resistance. On average, the peak anodic current was reduced by over 300 mV, the passivation potential was reduced, and the pitting potential was increased by over 1000 mV in 0.01 M NaCl. Ti + C and Ti + N implantations increased the load-carrying capacity in lubricated scuffing tests by 60% and 40% respectively. Ta produced no improvement in scuffing resistance. Ti + N implantation increased the hardness by 25% over the unimplanted steel and both Ti + C and Ta implantation reduced the surface hardness. Fretting wear was reduced only slightly in the Ta implanted sample and increased in both the Ti + C and Ti + N implanted samples with the latter showing 4–5 times the weight loss as the unimplanted sample. The correlation between fretting and hardness supports a mechanism in which the hard surface layer breaks into fine particles which act as an abrasive under the intense load of the balls.

1. Introduction

It has been widely demonstrated that ion implantation can alter the mechanical properties and corrosion behavior of many alloys. Of particular importance are the bearing steels such as AISI M50 and 52100. Service application often requires the use of these steels in aggressive environments or under severe localized wear modes. Applications require selection of the proper implant to improve the property which is responsible for in-service degradation. Implantation of Ti and C or Cr and Mo into M50 steel are both successful, but for different reasons. The main benefit of implantation consisting of Ti and C is believed to be the reduction in the friction coefficient by the formation of an amorphous phase [1, 2]. The decrease in friction under lubricated test conditions has been attributed to enhanced wetting characteristics of the interface which promotes hydrodynamic flow and inhibits surface contact [3]. The beneficial effect of a Cr and Mo implantation is due to a different reason. In a corrosive environment such as seawater, Cr imparts passivity to the bearing and Mo inhibits pitting of the passive film by the chloride ions [4].

Another severe wear process is fretting, or surface damage caused by low-amplitude oscillatory sliding between two contacting surfaces. Fretting is a complicated process involving the effect of contact conditions, environmental conditions and material properties [5]. Since fretting is intimately related to wear, corrosion and fatigue [6, 7], increasing the resistance to fretting is best accomplished by surface modifications which address these other degradation mechanisms. The problem at hand is the fretting of AISI 52100 and 1070 bearings by low amplitude oscillatory motion of the balls. Ion implantation is explored as a possible means of addressing this issue. Specifically, three implantation treatments have been selected: Ta, Ti + C and Ti + N implantation into 52100 and 1070 steels. To date, very little work has been done to explore the potential role of implantation on fretting. Therefore, implantations are selected on the basis of their effectiveness in improving wear, fatigue and corrosion of bearing steels. Ti + C has been shown to improve wear behavior, as previously

0257-8972/94/$7.00
SSDI 0257-8972(94)07019-N

mentioned. Ti+N has been very successful in reducing wear and corrosion when applied as a surface coating. Finally, Ta is very effective in improving the corrosion behavior of steels. Since fatigue spalling is improved by a reduction in friction and the introduction of compressive stresses, all implantations are expected to contribute to mitigation of this degradation mode.

2. Experiment

2.1. Materials

The materials were supplied in three forms: corrosion coupons 16 mm (0.625 inch) in diameter by 3 mm (0.125 inch) thick, wear disks 38 mm (1.5 inch) in diameter by 6 mm (0.25 inch) thick, and frettage test bearing races 35 mm (1.375 inch) in diameter by 4 mm (0.16 inch) thick. The corrosion and wear disks were made from both AISI 52100 (Fe–1.5Cr–1C–0.3Mn–0.2Si) or 1070 (Fe–(0.8–1.1)Mn–0.7C–(0.1–0.15)Cr) steels in the hardened and tempered condition. The heat treatment consisted of a soak at 843 °C (1550 °F) for 45 min followed by an oil quench and a tempering treatment at 232 °C (450 °F) for 1 h. The resulting hardness of the samples was R_c 59. The bearing races were made out of 52100 only and were annular in shape with an inner diameter of 16 mm, a thickness of 4 mm, and a curved bearing raceway. Their hardness was R_c 59 as well. The corrosion and wear disks received a final mechanical polish consisting of 1 μm diamond paste, and the bearing races were used in the as-received condition.

2.2. Implantation

Implantations were conducted on corrosion and wear disks of alloys 1070 and 52100 and on the curved bearing raceway of the alloy 52100 races. Implantations consisted of three types: Ti+C which was 3×10^{17} Ti^+ cm^{-2} at 120 keV followed by 1.5×10^{17} C^+ cm^{-2} at 40 keV, Ta which consisted of 1×10^{17} Ta^+ cm^{-2} at 140 keV, and Ti+N which consisted of 3.1×10^{17} Ti^+ cm^{-2} at 180 keV and 1.55×10^{17} N_2^+ cm^{-2} at 120 keV (assumed to be equivalent to 3.1×10^{17} N^+ cm^{-2} at 60 keV). Ti+C and Ta implantations were conducted at SPIRE Corporation and the Ti+N implantation was performed at the Michigan Ion Beam Laboratory (MIBL) at the University of Michigan. Vacuums in both cases ranged from mid 10^{-6} to low 10^{-7} Torr. So as not to disturb the metallurgical microstructure by beam heating, beam currents were limited to 1 μA cm^{-2}. In all cases, the beam was rastered across the sample at an angle normal to the plane of the sample. In the case of the bearing races, this resulted in a 0° implantation angle only at the bottom of the bearing track, which is appropriate for the frettage test procedure. The energies of the Ti+C and Ti+N were chosen to result in coincidence of the peaks of the implanted profiles. The results of Hubler *et al.* [8] were used to guide the selection of dose for both implants. The energy of the Ta implantation was set at the maximum achievable and the dose was chosen based on corrosion results from Hubler *et al.* [8].

2.3. Composition analysis

The composition of the implanted surfaces was analyzed using Rutherford backscattering spectrometry (RBS) and X-ray photoelectron spectroscopy (XPS). RBS was performed using 2 MeV He^{2+} in the Tandetron accelerator at the MIBL. Analysis of the Ta implantation was straightforward since the mass of Ta is greater than that of the substrate. Analysis of the Ti+C and Ti+N implantations was aided by the use of the PROFILE code [9] to determine the composition profile of the implanted species. XPS was performed on a Perkin–Elmer PHI 5400 X-ray photoelectron spectrometer by surface depth profiling using 3 keV Ar^+ ions.

2.4. Corrosion

Potentiodynamic polarization scans were conducted in either 0.5 N sulfuric acid or 0.01 M NaCl in pH 6.0 phosphate buffer on corrosion disks that were lacquered off to expose a small (0.02–0.2 cm^2) area to the solution. Polarization scans were begun soon after immersion in the acid solution since reduction of the air-formed film occurred quickly at the open-circuit potential. However, the reduction of the film was much slower in the chloride solution. As such the sample was held at a potential 250 mV below open-circuit for several minutes prior to performing polarization scans. Both solutions were deaerated prior to testing. Polarization scans were conducted at a rate of 1 mV s^{-1} and began at −1000 mV(SCE) in the chloride solution and at −10 mV(SCE) in the acid solution using a Princeton Applied Research (PAR) model 173 potentiostat with a model 276 digital interface linking it to an IBM personal computer.

2.5. Wear and hardness

The hardness of the unimplanted and implanted surfaces was measured using a Matsuzawa MXT70-UL Knoop hardness indenter with loads in the range 1–10 g. The wear behavior of the various surface treatments was determined by a scuffing test procedure. In this test, a stationary ball is pressed into contact with a rotating flat disk specimen. The contact load is determined by weights applied to the end of the bar to which the stationary slider is attached. The applied load can be controlled up to a maximum of 1300 N. The ball, which is taken from a bearing, slides on a flat surface in a direction parallel to the disk surface at a speed of 0.72 m s^{-1}, controlled with a d.c. servo motor. Mineral oil was used as lubricant. A conventional step loading method

was used in which the applied load is increased after sliding for a fixed amount of time (5 min) with a constant applied load. The coefficient of friction was measured as a function of load.

2.6. Fretting

Frettage tests were conducted in a Fafnir model 11636 friction oxidation tester which consists of a chuck containing two test bearings. Each bearing consists of a pair of bearing races and nine, 6 mm (0.25 inch) diameter balls made of AISI 52100. The test load is applied by tightening the castle nut until the calibrated coil spring is compressed to the step or shoulder on the chuck top shaft. When assembled, one race or washer of each of the two bearing sets mounted in the oscillating bearing seat is free to oscillate with respect to their fixed mates mounted in the chuck top and base. An eccentric mounted on the motor shaft and connected to the oscillating bearing seat crank by means of a connecting rod makes the small angle of oscillation possible.

Test bearing races were cleaned and weighed to the nearest 0.1 mg before being assembled with the test grease (Esso Nebula EP1 Batch 2) and mounted in the test equipment. The bearings were then tested at a constant temperature of −32 °C (0 °F), a frequency of 30 Hz and a force of 2446 N (550 lbs) for 22 h. On removal, the races were again cleaned and weighed with the fretting wear determined by the weight loss experienced by the races.

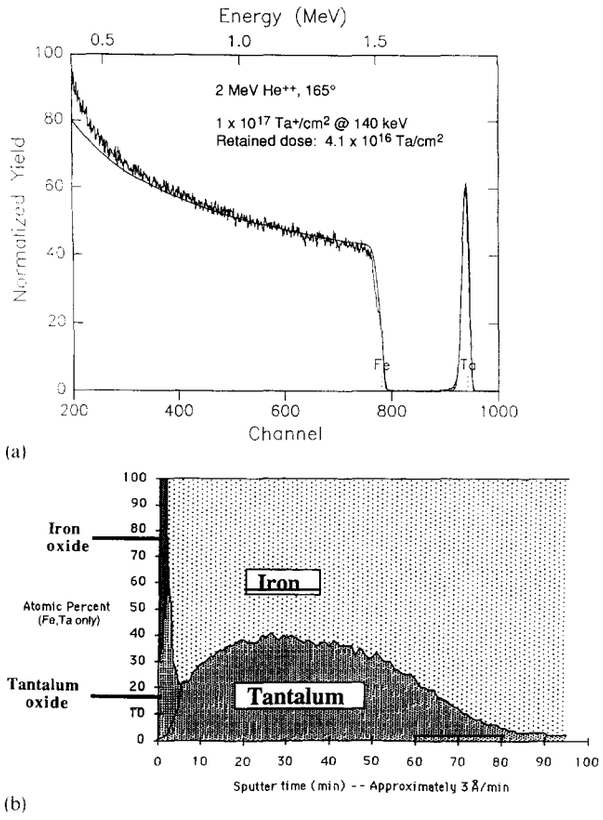

Fig. 1. RBS spectrum (a) and composition profile as determined by XPS (b) for Ta implanted 52100 steel.

3. Results and discussion

3.1. Composition

RBS spectra and composition profiles as determined by XPS for the three implantations are shown in Figs. 1–3. The RBS plots, Figs. 1(a)–3(a), show both the measured spectrum and the RUMP simulation giving the best fit. The simulation was based on composition *vs.* depth profiles determined using the PROFILE code, and adjusting the sputtering coefficient until the best fit was achieved. The retained dose is also shown for each implanted specie. Figures 1(b)–3(b) show the results of XPS depth profiling using 3 keV Ar^+ at a current density of about 8 μA cm^{-2} for Ta and Ti+C and 80 μA cm^{-2} for Ti+N. A sputtering rate of 3 Å min^{-1} was assumed in the conversion from sputter time to depth for Ta and Ti+C and 30 Å min^{-1} for Ti+N.

RBS and XPS results both agree in the amount and distribution of Ta. The retained Ta dose is 4.1×10^{16} cm^{-2} or 41% of the nominal dose (which yields a sputtering coefficient for Ta of about 2.7) and it is distributed in the form of a truncated Gaussian distribution with a peak at about 7.5 nm. The Ti+C implantation resulted in a retained dose of approximately 1.7×10^{17} Ti cm^{-2} (57% of nominal) but a much larger amount of C, perhaps picked up from the vacuum during deposition. RBS, XPS and PROFILE fitting all agree. The estimated sputtering yields are 2.5 for Ti and 0.6 for C. A fit to the RBS spectrum using PROFILE gives a retained dose of 2.2×10^{17} Ti cm^{-2} (0.71%) and an N dose which appears to be equivalent from XPS analysis. However, the RBS spectrum could only be fitted by assuming a significant concentration of a light element in the surface layers, perhaps C. The lower retained Ti dose (in per cent) in the Ti+C implant *vs.* the Ti+N implant is expected owing to the lower implantation energy of Ti in the Ti+C implantation. Overall, element concentrations and distributions determined using RBS directly, the PROFILE code and XPS agree reasonably well.

3.2. Corrosion

Potentiodynamic polarization experiments in 0.5 N sulfuric acid showed only minor differences in electrochemical behavior between as-received and (Ti+C or Ta) implanted samples, Fig. 4. Note that the scans are very reproducible and the data on the unimplanted sample agree well with those of Hubler *et al.* [8] on M50 steel. Hubler showed that Ta implantation results

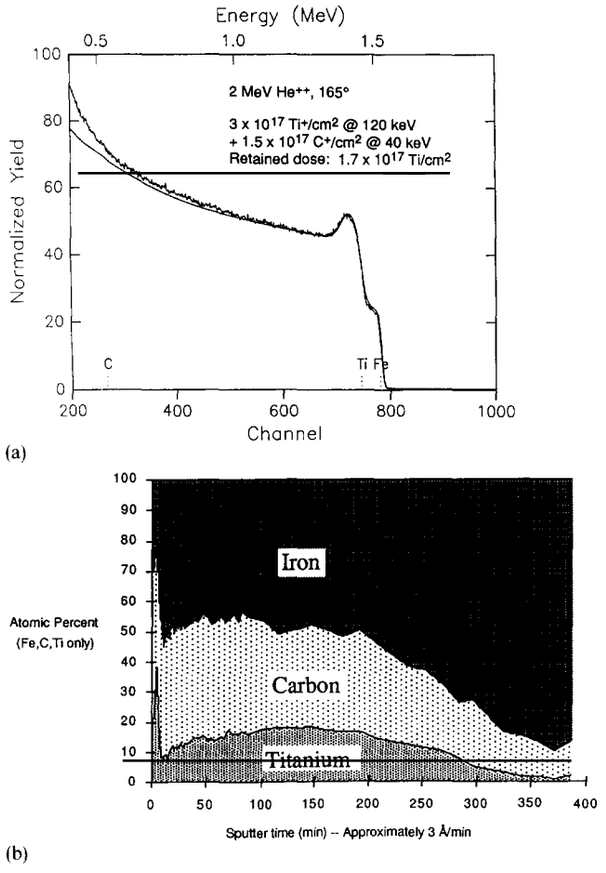

Fig. 2. RBS spectrum (a) and composition profile as determined by XPS (b) for Ti+C implanted 52100 steel.

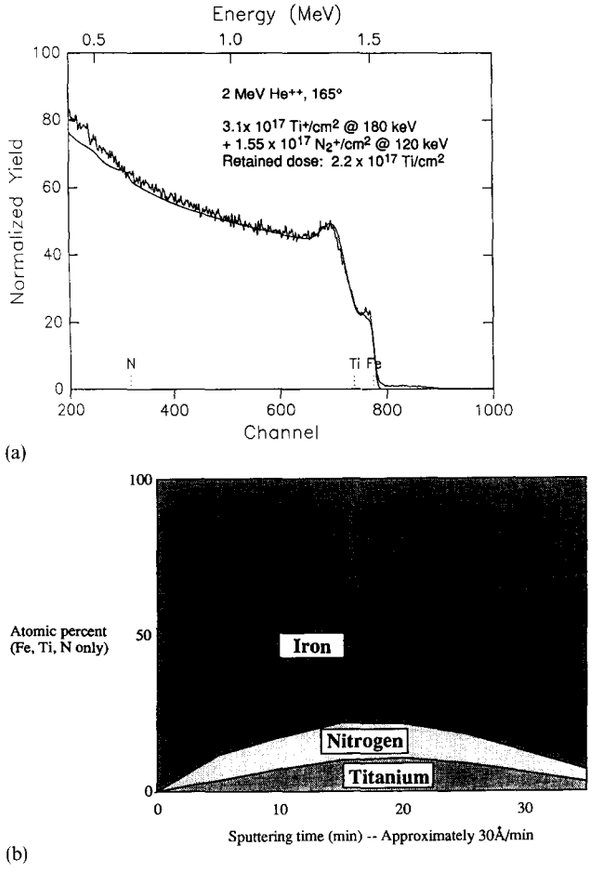

Fig. 3. RBS spectrum (a) and composition profile as determined by XPS (b) for Ti+N implanted 52100 steel.

in a smaller anodic peak and a decrease in the potential at which the current begins to increase in the transpassive region. The same is true of these results but the effect is not as large. Figure 4 shows that both the Ta and Ti+C implanted samples exhibit a lower anodic peak (by about 10 times), an approximately 100 mV drop in the passivation potential and little change in the passive region or the onset of the transpassive region. Analysis of the exposed surfaces indicates that the unimplanted sample corrodes uniformly, resulting in a black corrosion product. However, both the Ti+C and Ta implanted samples retained polishing scratches and were etched in some regions, while others remained reflective. The reduction in the peak anodic current and the decrease in the passivation potential are attributed to the formation of a Ta_2O_5 film by selective dissolution of Fe and reprecipitation of Ta.

Polarization results in 0.1 M buffered NaCl solution are more striking. The unimplanted samples were severely pitted owing to the low pitting potential (−100 mV (SCE)), while all implantations were effective in reducing the size of the anodic peak, improving the passivation behavior and raising the pitting potential, Fig. 5. Both Ta and Ti+C implantations increased the open-circuit potential by about 300–350 mV, dropped the anodic peak by 100 times and increased the pitting potential by about 1300–1400 mV. The Ti+N implantation did not change the open-circuit potential but decreased the peak anodic current density by more than 100 times and increased the pitting potential by 1400 mV. Results for Ta agree extremely well with those of Hubler *et al.* [8] and Nielsen *et al.* [10]. Results of Ti+C implantation also agree with Hubler *et al.* [2] and the results of TiN are in line with those observed by others [11]. Pitting was extremely severe in the unimplanted sample, but the sample surface remained bright and free from localized attack in all the implanted surfaces. The one exception was the Ta implantation which showed some pitting, but this may have been due either to the shallow depth of the implant layer relative to the surface roughness or to polarization above the pitting potential. Improved corrosion resistance is attributed to the formation of Ta_2O_5 in the case of Ta implantation and perhaps to amorphization of the surface layers.

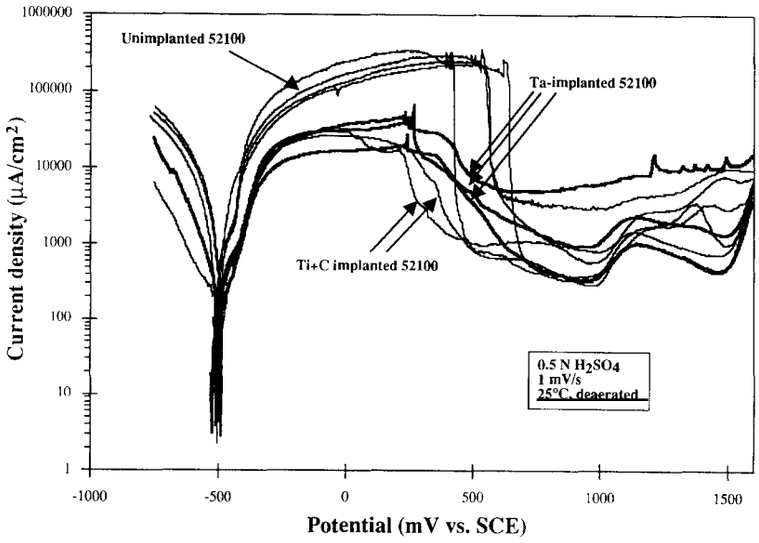

Fig. 4. Potentiodynamic polarization plots of unimplanted, Ta implanted and Ti+C implanted 52100 steel in deaerated 0.5 N sulfuric acid at 25 °C and a scan rate of 1 mV s^{-1}.

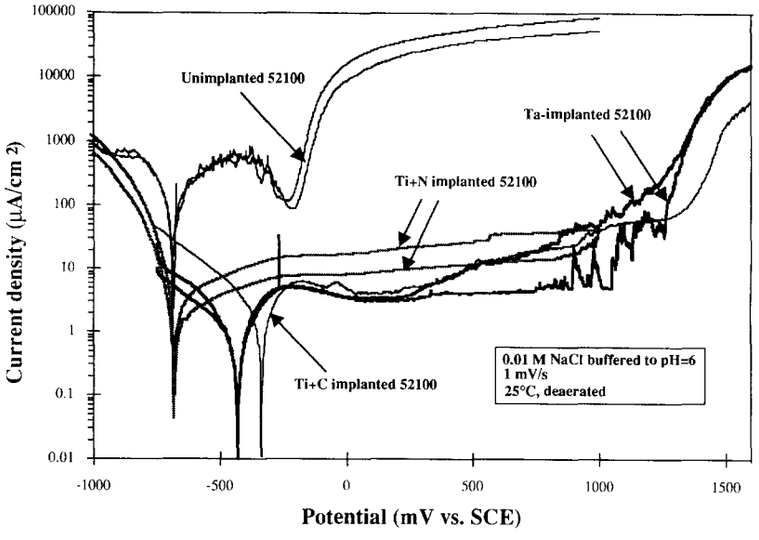

Fig. 5. Potentiodynamic polarization plots of unimplanted, Ta implanted, Ti+C implanted and Ti+N implanted 52100 steel in deaerated 0.01 M NaCl buffered to pH 6 at 25 °C and a scan rate of 1 mV s^{-1}.

3.3. Wear and hardness

Scuffing test results are summarized in Fig. 6 which plots the coefficient of friction as a function of the applied load. These results show that both Ti+C and Ti+N implantation were effective in increasing the load-carrying capacity over that for unimplanted steel. Ta implantation, however, provided no improvement in the load-bearing capacity, in contrast to the results of Hubler *et al.* [8]. The load-carrying capacity in the scuffing test is attributed either to the hardness of the surface layer or the change in friction coefficient. This hard, thin layer minimizes plowing and subsurface deformation and hence increases the effectiveness of running-in, thus increasing scuffing resistance. Observed increases in the load-carrying capacity agree fairly well with the measured hardness following implantation, Table 1. Ti+N implantation increases the surface hardness as expected, producing an increase in the scuffing resistance. Both Ti+C and Ta implantation, however, reduce the surface hardness, in agreement with Oliver *et al.* [12]. However, while Ti+C was effective in increasing the scuffing resistance, Ta was not. Ti+C implantation is known to

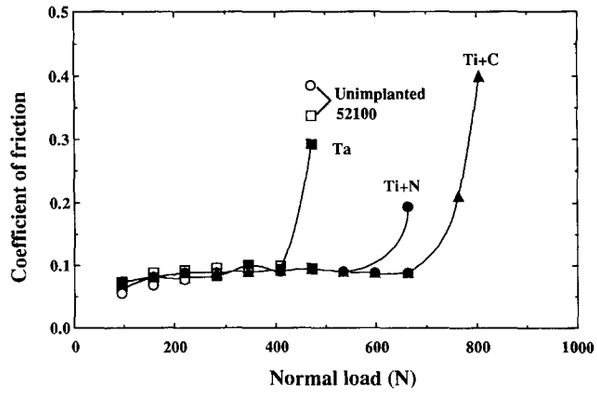

Fig. 6. Coefficient of friction as a function of the normal load in a lubricated step-load test on unimplanted, Ta implanted, Ti+C implanted and Ti+N implanted 52100 steel.

TABLE 1. Normalized hardness of implanted samples

Load (g)	Ta	Ti+C	Ti+N
10	0.73	0.79	0.98
1	0.80	0.82	1.25

Hardnesses are relative to the unimplanted values.

reduce the friction coefficient, but no significant change was observed in these tests. Ta implantation is not expected to result in either a harder film or a lower friction coefficient and this is consistent with the observed results.

3.4. Fretting

Results of fretting tests are given in Fig. 7. The results are somewhat ambiguous in that there is a large amount of scatter in the data. Inspection of the bearing pattern following testing revealed that misalignment and walking bearings contributed to some of the observed scatter in the data. Walking of bearings affected three of the four unimplanted samples and the other showed indications of load spring misalignment. Walking occurred in both of the Ti+N implanted pairs and in one of the four Ta implanted pairs. There was also some evidence of set screw misalignment in several of the pairs. Although the scatter is great, certain trends can be identified. First, Ta implantation resulted in fretting wear that was on par or slightly improved over the unimplanted bearings. The Ti+C implantation resulted in greater fretting wear, as did the Ti+N implantation. There appears to be an inverse correlation between fretting wear resistance and surface hardness. This is not totally unexpected. A hard thin layer can be a source of abrasive wear particles in a fretting test. The difference in the role of this layer in sliding wear and fretting wear is the sliding distance. In sliding wear, sliding distances are large and oil constantly sweeps away wear debris before the next pass. However, in the case of fretting caused by high frequency oscillations, the sliding distance is extremely small and wear particles can become trapped between the contact area, acting as hard abrasive particles and promoting fretting wear [13]. The increased hardness of the implanted surface layers may also reduce the fracture resistance, thus increasing the rate of wear particle formation. Finally, oxides which are beneficial in scuffing tests may be detrimental in fretting, as fretting in a non-oxidizing environment has been found to be less severe than in an oxidizing environment [13].

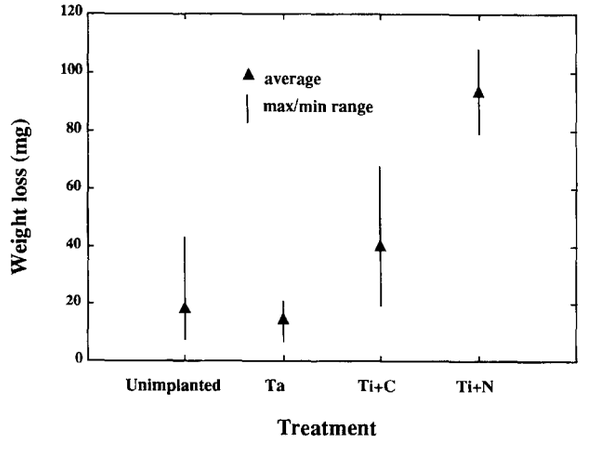

Fig. 7. Weight loss in a fretting test using a Fafnir model 11636 tester and Esso Nebula EP1 batch #2 grease on unimplanted, Ta implanted, Ti+C implanted and Ti+N implanted bearings.

4. Summary

The results indicate that all implantations were very effective in improving the corrosion resistance. On average, Ti+C, Ti+N and Ta implantations reduced the peak anodic current by greater than or equal to 300 mV, reduced the passivation potential, and increased the pitting potential by over 1000 mV. This resulted in the formation of a protective passive film and a high resistance to pitting in both 0.5 M H_2SO_4 and 0.1 N buffered (pH 6) NaCl solutions. Ti+C and Ti+N implantations significantly increased the wear resistance in a lubricated step-load scuffing test by 60% and 40% respectively. Ta produced no improvement in the wear resistance. Ti+N implantation increased the hardness by about 25% and both Ti+C and Ta implantation reduced the surface hardness. Fretting wear was reduced only slightly in the Ta implanted sample and increased in both the Ti+C and Ti+N implanted samples with the latter showing 4–5 times the weight loss as the unimplanted sample. The fretting results correlate well with hardness, supporting a mechanism in which the

hard surface layer breaks into fine particles which act as an abrasive under the intense load of the balls. Owing to the very small sliding distance, the wear debris cannot be swept away and ultimately is responsible for the observed weight loss.

Acknowledgments

The authors gratefully acknowledge the Delco Chassis Division of General Motors Corporation for their financial support. The authors also acknowledge the many helpful discussions with Mr. Ken Neer of Delco Chassis and Dr. Dale Alexander of Argonne National Laboratory and the Michigan Ion Beam Laboratory at the University of Michigan.

References

1 C. A. Carosella, I. L. Singer, R. C. Bowers and C. R. Gossett, *Mater. Sci. Eng.*, *69* (1985) 103.
2 G. K. Hubler, P. Trzaskoma, E. McCafferty and I. L. Singer, in V. Ashworth, W. A. Grant and R. P. M. Proctor (eds.), *Ion Implantation into Metals*, Pergamon, New York, 1982, p. 24.
3 P. Sioshansi and J. J. Au, *Mater. Sci. Eng.*, *69* (1985) 161.
4 C. R. Clayton, W. K. Chan, J. K. Hirvonen, G. K. Hubler and F. R. Reed, in E. McCafferty, C. R. Clayton and J. Oudar (eds.), *Fundamental Aspects of Corrosion Protection by Surface Modification*, Electrochemical Society, Pennington, NJ, 1984, p. 17.
5 J. J. O'Connor, in R. B. Waterhouse (ed.), *Fretting Fatigue*, Applied Science, London, 1981, p. 23.
6 W. C. Oliver, R. Hutchings and J. B. Pethica, *Metall. Trans. A*, *15* (1984) 2221.
7 V. Ashworth, R. P. Procter and W. A. Grant, The application of ion implantation to aqueous corrosion. In *Treatise on Materials Science and Technology*, Vol. 18, Academic Press, New York, 1980, p. 175.
8 G. K. Hubler, I. L. Singer and C. R. Clayton, *Mater. Sci. Eng.*, *69* (1985) 203.
9 S. N. Bunker and A. J. Armini, *Nucl. Instrum. Methods B*, *39* (1989) 7.
10 B. R. Nielsen, B. Torp, C. M. Rangen, M. H. Simplicio, A. C. Colnsiglieri, M. F. DaSilva, F. Paszti, J. C. Soares, A. Dodd, J. Kinder, M. Pitaval, P. Thevenard and R. G. Wing, *Nucl. Instrum. Methods B*, *59–60* (1991) 772.
11 E. I. Meletis, A. Erdimer and R. F. Hochman, in R. F. Hochman (ed.), *Ion Plating and Implantation*, American Society for Metals, Metals Park, OH, 1986, p. 173.
12 W. C. Oliver, R. Hutchings, J. B. Pethica, I. L. Singer and G. K. Hubler, in G. K. Hubler, C. W. White, O. W. Holland and C. R. Clayton (eds.), *Ion Implantation and ion Beam Processing of Materials*, Materials Research Society Symp. Proc., Vol. 27, Elsevier, New York, 1984, p. 603.
13 J. E. Elder, R. Thamburaj and P. C. Patnaik, *Int. Mater. Rev.*, *33* (6) (1988) 289.